ACE2 is necessary for SARS-CoV-2 infection and sensing by macrophages but not sufficient for productive viral replication

Larisa I Labzin[1,2,3]*, Keng Yih Chew[4], Xiaohui Wang[1,2], Tyron Esposito[1,2], Claudia J Stocks[1,2], James Rae[1,9], Teodor Yordanov[1], Caroline L Holley[1,2], Stefan Emming[1,2], Svenja Fritzlar[5], Francesca L. Mordant[5], Daniel P. Steinfort[6,7], Kanta Subbarao[5,8], Anne K Lagendijk[1], Robert Parton[1,9], Kirsty R. Short[3,4], Sarah L. Londrigan[5, #], Kate Schroder[1,2,3,4, #].

[#]These authors contributed equally

[*] Correspondence should be addressed to l.labzin@uq.edu.au

[1]Institute for Molecular Bioscience (IMB), The University of Queensland, Brisbane, QLD, Australia

[2]IMB Centre for Inflammation and Disease Research, The University of Queensland, Brisbane, QLD, Australia

[3]Australian Infectious Diseases Research Centre, The University of Queensland, Brisbane, QLD, Australia

[4]School of Chemistry and Molecular Biosciences, The University of Queensland, Brisbane, QLD, Australia

[5]Dept of Microbiology and Immunology, The University of Melbourne at the Peter Doherty Institute for Infection and Immunity, Melbourne, Victoria, Australia.

[6]Department of Medicine, The University of Melbourne, Parkville, Victoria, Australia

[7]Department of Respiratory Medicine, Royal Melbourne Hospital, Parkville, Victoria, Australia

[8] WHO Collaborating Centre for Reference and Research on Influenza, Victorian Infectious Diseases Reference Laboratory, at The Peter Doherty Institute for Infection and Immunity, Melbourne, Victoria, Australia.

[9]Centre for Microscopy and Microanalysis, The University of Queensland, Brisbane, QLD, Australia

Abstract

Macrophages are a major source of pro-inflammatory cytokines in COVID-19. How macrophages sense the causative virus, SARS-CoV-2, to drive cytokine release is, however, unclear. Here, we show that human macrophages do not directly sense and respond to infectious SARS-CoV-2 virions because they lack sufficient ACE2 expression to support virus entry and replication. Over-expression of ACE2 in human macrophages permits SARS-CoV-2 entry and early-stage replication and facilitates macrophage pro-inflammatory and anti-viral responses. ACE2 over-expression does not, however, permit the release of newly synthesised virions from SARS-CoV-2-infected macrophages, consistent with abortive replication. Release of new, infectious SARS-CoV-2 virions from ACE2 over-expressing macrophages only occurred if anti-viral mediator induction was also blocked, indicating that macrophages restrict SARS-CoV-2 infection at two stages of the viral life cycle. These findings resolve the current controversy over macrophage-SARS-CoV-2 interactions and identify a signalling circuit that directly links macrophage recognition of SARS-CoV-2 to restriction of viral replication.

One sentence summary:

ACE2 is necessary for SARS-CoV-2 infection and sensing by macrophages but not sufficient for productive viral replication.

Main Text

INTRODUCTION

Effective host defence against infection relies on accurate and timely immune detection. Accumulating evidence suggests that severe COVID-19, caused by Severe Acute Respiratory Syndrome Coronavirus 2 (SARS-CoV-2) infection, results from a failure of early host interferon signalling to control the virus, followed by exacerbated pro-inflammatory responses driving tissue damage. Airway epithelial cells, the primary target for SARS-CoV-2 infection (*1*), respond by releasing both anti-viral and pro-inflammatory cytokines (*2*, *3*). Airway-resident or newly recruited macrophages also appear to be a key source of pro-inflammatory cytokines in severe COVID-19 (*4*, *5*), with macrophage-derived cytokines implicated in the severe pathology seen in patients (*6*–*9*)

SARS-CoV-2, belonging to the *Coronaviridae* family, is an enveloped, single-stranded RNA virus with a positive-sense genome. Many human respiratory viruses, including SARS-CoV-2, infect epithelial cells lining the upper and lower airways, resulting in productive replication and the release of newly synthesised infectious viral particles. The virus Spike (S) glycoprotein facilitates entry into target epithelial cells by binding to surface expressed angiotensin-converting enzyme 2 (ACE2) receptor (*10*). The well characterised ACE2-Spike interaction exposes a critical S cleavage site (S2) that can then be cleaved by the host serine protease transmembrane protease, serine 2 (TMPRSS2), also expressed on the plasma membrane. This allows fusion of the viral and cellular membranes, followed by release of viral RNA directly into the cytoplasm (reviewed by ((*11*) and (*12*)). SARS-CoV-2, particularly the omicron variant, can also attach to ACE2 and enter cells via the endocytic pathway, where S protein is cleaved by endosomal proteases to allow fusion between the viral and endosomal membranes (*13*). The infecting RNA genome is then translated into two large polyproteins that can be proteolytically processed to generate individual viral proteins for replication and transcription. New virions are assembled in the endoplasmic reticulum and Golgi of the host cell, and are secreted from the cell via exocytosis or through a lysosomal egress pathway (*12*). The SARS-CoV-2 replication cycle has primarily been characterised in epithelial cells and cell lines. How this may differ in other potentially susceptible cell types, including immune cells, remains unclear.

Macrophages are sentinel innate immune cells that are present in the airway during respiratory viral infection and are critical for effective host defence. In contrast to epithelial cells, however, human macrophage infection with many respiratory viruses (including seasonal influenza A viruses (*14*), and rhinovirus (*15*)) is abortive, despite macrophages being susceptible to the early stages of infection (entry and synthesis of new viral RNA and protein). In addition to acting as a viral 'dead end' to limit viral dissemination (*16*), macrophages can sense infectious virions, neighbouring cell infection and damage to drive anti-viral and pro-inflammatory cytokines, which control viral loads in many respiratory infections (*17–19*). The contribution of macrophages to potent and effective innate responses to control SARS-CoV-2 infection is controversial. While there is consensus that SARS-CoV-2 infection of human monocyte derived macrophages (HMDM) is abortive (*3*, *8*, *9*, *20–22*), some studies report that macrophages are susceptible to the early-stages of SARS-CoV-2 infection (i.e. viral entry) and replication, (i.e. viral RNA replication and protein synthesis) (*8*, *9*, *20*), while others report no viral entry into macrophages (*3*, *22*). Accordingly, whether macrophage susceptibility to SARS-CoV-2 is required to trigger inflammatory and anti-viral signalling is unclear, with multiple reports suggesting that macrophage infection triggers pro-inflammatory responses (*8*, *9*, *23*) while others report that infection does not activate macrophage inflammatory functions (*3*, *22*). In this study, we investigated whether macrophages sense infectious SARS-CoV-2 virions to trigger pro-inflammatory and anti-viral mediator release. In so doing, we resolve the controversy of whether primary human monocyte-derived and airway-resident macrophages are susceptible and permissive to SARS-CoV-2 infection.

RESULTS

Human monocyte-derived macrophages (HMDM) do not release pro-inflammatory cytokines or anti-viral mediators upon SARS-CoV-2 exposure

During infection with SARS-CoV-2, monocytes are rapidly recruited from the circulation to the infected lungs (*4*), where they differentiate into macrophages that encounter the virus. To model this, we incubated HMDM with SARS-CoV-2 and monitored macrophage responses by quantifying cytokine release in cellular supernatants. We challenged HMDM with a high dose of SARS-CoV-2 (multiplicity of infection; MOI 5) for 24h without removing the virus to allow maximal macrophage responses. SARS-CoV-2 did not trigger CXCL10, IL-6 or

TNF release *in vitro* (**Figure 1A**), despite reports indicating that these cytokines circulate at high levels *in vivo* during SARS-CoV-2 infection (*24*, *25*). By contrast, HMDM showed a robust secretory response to synthetic viral mimetics such as the toll-like receptor (TLR) 7/8 ligand, R848 (TNF, IL-6) and the melanoma differentiation-associated protein 5 (MDA5) ligand, transfected poly I:C (pIC) (CXCL10) (**Figure 1A**). mRNA analyses revealed that SARS-CoV-2 did not upregulate HMDM expression of *Ifnb1*, *Ifnl1*, *Cxcl10*, *Il6*, *Tnf* or *Il1b* at 2h or 24h post-infection (p.i.), at either low (0.5) or high (5) MOI, while these genes were robustly induced by R848 and pIC (**Figure 1B**). Thus, HMDM do not respond to SARS-CoV-2 exposure *in vitro*, even at the high MOI of 5.

HMDM and primary human airway macrophages do not support infection and replication of SARS-CoV-2

The failure of primary HMDM to respond to SARS-CoV-2 exposure contrasts with previous reports that demonstrated SARS-CoV-2 induces the expression of cytokine mRNAs (including *Il6*, *Cxcl10*, and *Tnf*) in HMDM (*8*, *9*, *23*, *26*). We therefore investigated whether the HMDMs generated in this study were susceptible to SARS-CoV-2 infection and replication. SARS-CoV-2-permissive Calu3 epithelial cells were included as a positive control for viral infection and replication. The viral inoculum was left on the cells as before to maximise uptake of SARS-CoV-2 virions by HMDM. Calu3 cells were susceptible to infection with both high and low dose infection (MOI 5 and 0.5) as we observed an increase in cell-associated viral RNA between 2h (indicative of input virus) and 24h post-infection, indicating newly synthesized viral RNA and active replication (**Figure 2A**). In contrast, cell-associated viral RNA levels did not increase in HMDM infected with either MOI over the same time (**Figure 2B**). Further, newly synthesised viral protein was evident in Calu3 control cells, where viral nucleoprotein (NP) expression increased from 2h to 72h in Calu3 (**Figure 2C**). In contrast, HMDM did not support the production of newly synthesised viral NP, where NP expression was barely detectable at 24h post-infection, compared to detectable NP associated with input virus at 2h post-infection (**Figure 2D**). These data indicate that HMDM are not susceptible to SARS-CoV-2 infection and do not support the early stages of viral replication, including the production of newly synthesized viral RNA and protein.

The lung-resident macrophage population are immune sentinels of the airways, with different origins and properties from those of HMDM (*27*). Along with airway epithelial cells, airway

macrophages are primary targets for infection by various respiratory viruses. We next investigated whether this lung-resident macrophage population differed from HMDM in their susceptibility to SARS-CoV-2 infection and replication. Airway macrophages, obtained from bronchoalveolar lavage (BAL) and considered to be representative of resident lung macrophages, were isolated from three donors and infected with SARS-CoV-2 at an MOI of 1. SARS-CoV-2-infected BAL macrophages showed no increase in cell-associated viral RNA (indicative of the early stages of virus replication) between 2h and 48h post-infection, in contrast to the SARS-CoV-2-susceptible control cell line VERO E6 (**Figure 2E**). An increase in viral RNA isolated from cell-free VERO E6 supernatants between 2 and 24h post-infection was indicative of productive viral replication, with release of newly synthesized viral RNA from infected cells, but this was not observed in supernatants of SARS-CoV-2 infected BAL macrophages (**Figure 2F**). These data indicate that as for HMDM, airway macrophages are not permissive to at least the early stages of SARS-CoV-2 infection and replication.

Macrophage susceptibility to SARS-CoV-2 requires ACE2 expression

Macrophages may restrict SARS-CoV-2 replication at different stages in the viral life cycle, including during entry. As ACE2 is the primary receptor facilitating SARS-CoV-2 attachment to host cells, we next investigated whether ACE2 expression could be a determining factor in macrophage resistance to SARS-CoV-2 infection. We assessed ACE2 mRNA and protein levels by qPCR and immunoblot, and observed low *Ace2* mRNA expression, and no ACE2 protein expression in HMDM isolated from 4 individual donors (**Figure 3A, B**), even when HMDM were treated with IFNβ (**Figure 3B**). Similarly, ACE2 protein was not detected in airway macrophages isolated from BAL macrophages of 3 individual donors (**Figure 3C**). We used lentiviral transduction to overexpress either ACE2 (untagged) or a control protein (mScarlet, mSc) in the THP-1 monocyte cell line and differentiated these to macrophage-like cells with phorbol-myristate-acetate (PMA). We confirmed that ACE2 overexpression in THP-1 cells resulted in readily detectable ACE2 mRNA and protein **(Figure 3A, 3B).** The surface protease TMPRSS2, which is required for S protein cleavage, was also readily detected at the protein level in HMDM and THP-1-ACE2 cells **(Figure 3B).**

We next explored whether insufficient ACE2 expression is the primary block to SARS-CoV-2 replication in macrophages. We thus challenged THP-1-ACE2 with SARS-CoV-2 (MOI 0.5 and 5) and compared viral replication and release to THP-1-mSc and Calu3 control cells. There was a significant increase in cell-associated viral RNA in THP-1-ACE2 cells at 24h p.i. at both MOIs, before plateauing from 24 to 72h p.i., indicating cell susceptibility and early-stage viral RNA replication (**Figure 3D, 3E)**. By contrast, viral RNA levels did not increase in the THP-1-mSc control cells at any timepoint (**Figure 3D, 3E**), similar to observations in HMDM and BAL macrophages **(Figure 2B, 2E, 2F).** As expected, in Calu3 cells which support viral replication and virion release (*28*), SARS-CoV-2 RNA levels continued to increase over the time course (**Figure 3D, 3E**).

To determine whether the increased cell-associated viral RNA in THP-1-ACE2 cells was coupled to the release of infectious virions, we performed plaque assays on cell-free supernatants to measure release of infectious viral particles, represented by plaque forming units (PFU). Despite increased cell-associated viral RNA, we observed a decrease in infectious viral particles in THP-1-ACE2 cells at 48 or 72h p.i. compared with input virus levels at 0h (**Figures 3F, 3G**). Similarly, we observed a decrease in infectious viral particles in THP-1-mSC cell-free supernatants (**Figure 3F, 3G**). In contrast, Calu3 cells were productively infected at the low MOI (MOI 0.5) over the same time course, indicated by a significant increase in infectious viral particles present in cell-free supernatants between 0 and 72h p.i. **(Figure 3F)**, though at high MOI (MOI 5) detection of new infectious virions peaked at 24h (**Figure 3G**). This suggests that while some new virions are produced in THP-1-ACE2 cells, a secondary block may serve to limit virus production in these cells. Together, these data suggest that ACE2 expression is necessary for SARS-CoV-2 entry and new viral RNA synthesis in macrophages but is not sufficient to support productive viral replication. Thus, macrophages have two blocks to productive SARS-CoV-2 replication – lack of ACE2 expression, plus an additional mechanism downstream of viral entry and replication that limits release of infectious virions.

Macrophages can take up SARS-CoV-2 independently of ACE2

Additional SARS-CoV-2 entry receptors beyond ACE2 are reported, such as the C-type lectin receptors (CLRs) (*23*). As our assays to measure viral protein and RNA were unable to distinguish whether virus is intracellular or extracellular (Figure 2B,2D), we next determined

whether SARS-CoV-2 can still bind and enter HMDM, despite lack of ACE2 expression. We used transmission electron microscopy to determine the sub-cellular location of incoming virions. To capture these events, we used a high MOI of 20. HMDM (**Figure 4A, A'**) and THP-1-ACE2 (**Figure 4B**) showed internalised, intact virions within the phagosomal system after 1h infection. In THP-1-ACE2 cells but not HMDM, we also observed virions bound and potentially starting to fuse at the plasma membrane (**Figure 4C, C'**), and these were morphologically similar to the new structures being released from Calu3 at 72h p.i. (**Figure 4D**). As THP-1-ACE2 cells endogenously express TMPRSS2 (**Figure 3B,**), this suggests that THP-1-ACE2 cells may support viral fusion at the plasma membrane to deliver the viral genome and NP directly into the cytoplasm. Taken together, these results suggest that while HMDM can take up SARS-CoV-2 into phagosomal compartments, low ACE2 expression will preclude SARS-CoV-2 S processing and virus-cell membrane fusion, steps that are necessary for this virus to enter the cytoplasm.

Ectopic ACE2 expression potentiates macrophage inflammatory responses to SARS-CoV-2

During infection, cells can sense incoming virions in addition to newly synthesised viral RNA and proteins (*29–31*). Although we detected viral particles in HMDM phagosomal compartments at 1h p.i. (**Figure 4A'**), this did not correlate with HMDM activation upon SARS-CoV-2 challenge (**Figure 1A, 1B**), suggesting that virions in these compartments were not detected by the cell. Given that ACE2 overexpression in macrophages permits efficient SARS-CoV-2 entry and early-stage viral replication, we next assessed whether THP-1-ACE2 cells produce pro-inflammatory and anti-viral mediators upon SARS-CoV-2 challenge. THP-1-ACE2 cells strongly upregulated *Ifnb1*, *Ifnl1*, *Cxcl10 and IL-6* mRNA expression after infection with SARS-CoV-2 for 24h (at MOI 5, **Figure 5A**; or MOI 0.5, **Supp. Figure 5A**), correlating with increased SARS-CoV-2 viral RNA levels (**Figure 3E**). THP-1-mSc cells did not respond to SARS-CoV-2 challenge at either MOI (**Figure 5A, Supp Figure 5A)**, similar to HMDM (**Figure 1A, 1B**). We confirmed that viral sensing pathways were operational in both THP-1-ACE2 and THP-1-mSC, by stimulating MDA5 via pIC transfection (**Supp Figure 5B**). In Calu3 cells, both anti-viral (*Ifnb1*, *IfnL1*, *Cxcl10*) and pro-inflammatory (*Tnf*, *IL6*) gene induction peaked at 72h p.i. (at MOI 5, **Figure 5B**; MOI 0.5, **Supp Figure 5C**), consistent with published observations (*3*), and the rise in SARS-CoV-2 viral RNA expression (**Figure 3E,F**) and productive virus release (**Figure 3G,H**). Collectively, these

data suggest that ACE2 overexpression, which permits early-stage viral replication, is necessary for macrophage to sense infectious SARS-CoV-2 virions.

Blocking cytokine signalling in THP-1-ACE2 cells rescues productive virion release

Collectively, our findings suggest that human macrophages are not susceptible to infection with SARS-CoV-2 due to insufficient ACE2 receptor expression. Furthermore, while ACE2 overexpression can restore the permissivity of macrophages to the early stages of SARS-CoV-2 infection and replication, this does not result in productive viral infection, as infectious virions detected in the supernatant did not increase above the level of input virus (0h). It is possible that macrophage ACE2 expression is upregulated by stimuli present at sites of *in vivo* infection; if so, mechanisms by which ACE2-expressing macrophages restrict virus production may contribute to viral control *in vivo*. We thus explored potential mechanisms by which THP-1-ACE2 cells limit viral replication and release of new virions. Host cell death is proposed to limit release of SARS-CoV-2 infectious virions (*32*), and indeed, virus-challenged THP-1-ACE2 cells showed a modest but significant decrease (~20%) in viability compared to THP-1-mSc cells at 72 h p.i. at high MOI (MOI5, **Figure 6A**). Thus, cell death may limit virus release from THP-1-ACE2 when these cells encounter high viral loads.

We noted that the rapid and robust induction of Type I and III interferons, peaking at 24h p.i. in the THP-1-ACE2 cells, was delayed in the Calu3 cells (**Figure 5A, 5B**). Interferons can signal in both an autocrine and paracrine manner to activate an anti-viral state through the induction of interferon-stimulated genes, which act as restriction factors to limit viral infection (*33*). Indeed, Type I IFN is critical for abortive influenza A virus infection in murine macrophages (*16*). We hypothesised that interferon signalling in THP-1-ACE2 cells induces host factors that impede viral replication, precluding the release of productive virions. In contrast, the later induction of *Ifnb1* and *Ifnl1* in Calu3 cells, potentially through viral antagonism, likely allows for continuing viral replication and release. We tested this hypothesis using a TBK1 inhibitor (BX-795) to block virus-induced interferon induction and signalling (*34*) (**Figure 6B**). As expected, BX- suppressed pIC-induced expression of *Ifnb1* and *Ifnl1* and the interferon-stimulated gene *Cxcl10* (**Supp Figure 6A**). We next challenged THP-1-ACE2 and Calu3 cells with SARS-CoV-2 for 72 h, in the presence and absence of BX-795. BX-795 suppressed SARS-CoV-2-induced CXCL10 production from THP-1-ACE2

cells (**Figure 6C**) and restored productive virion release (**Figure 6D**). BX-795 did not affect productive virion release from Calu3 cells (**Figure 6E**), consistent with published observations (*3*). These findings indicate that, should macrophages upregulate ACE2 at sites of *in vivo* infection to permit SARS-CoV-2 entry, their capacity to rapidly induce interferon signalling suppresses viral replication to prevent viral dissemination. In sum, human macrophages protect themselves from productive SARS-CoV-2 infection through dual mechanisms: (1) low ACE2 expression, which prevents viral entry; and (2) rapid interferon-mediated anti-viral defence upon cell compromise.

DISCUSSION

A key question in SARS-CoV-2 pathogenesis is which host cells sense SARS-CoV-2 to trigger inflammatory cytokines and anti-viral mediator release. Given that macrophages are primary candidates for sensing and responding to SARS-CoV-2 (*7*), a second, unresolved question is whether SARS-CoV-2 can infect and productively replicate in human macrophages. This study elucidates the requirements for macrophages to sense and respond to SARS-CoV-2.

We demonstrate that primary HMDM do not respond to SARS-CoV-2 challenge, despite taking up virus through phagocytosis. We found that both BAL macrophages and HMDM do not express ACE2 protein, rendering them resistant to early-stage SARS-CoV-2 replication. In turn, ectopic expression of ACE2 rendered macrophages susceptible to SARS-CoV-2 entry and replication and able to mount ensuing robust pro-inflammatory and anti-viral responses. Intriguingly, ectopic ACE2 expression was not sufficient for macrophages to efficiently release new virions, and thereby increase viral titres. In this context, productive virion release can be rescued by disabling macrophage interferon production and signalling. Thus, macrophages have two key mechanisms that block productive SARS-CoV-2 infection: (1) lack of ACE2 prevents productive viral entry, and (2) in the presence of ACE2, viral sensing triggers rapid induction of potent anti-viral mediators to suppress the release of new virions.

Typically, a virus must directly infect and replicate in a cell to trigger the cytosolic pattern recognition receptors (PRRs), triggering so-called ‘cell intrinsic’ sensing, concomitant with a high level of threat to that cell. These cytosolic PRRs are ubiquitously expressed, and their activation leads to potent anti-viral mediator production (e.g. interferons-alpha, -beta, -

lambda), inflammatory cytokine signalling or cell death (*35*), all of which function to limit viral replication and warn neighbouring cells of imminent danger. In addition to these cytosolic PRRs, macrophages are also equipped with PRRs at distinct subcellular locations (e.g. cell surface, endosomes) to detect moderate threats, including signs of infection in neighbouring cells, viral pathogen-associated molecular patterns (PAMPs) or host danger-associated molecular patterns (DAMPs) in the extracellular milieu (*36*). This 'cell extrinsic' sensing reflects the local microenvironment, and through triggering cell-surface or endosomal PRRs, can induce a distinct suite of anti-viral and pro-inflammatory responses to 'cell intrinsic' sensing (*35*).

Our data indicate that primary HMDM do not directly respond to SARS-CoV-2 exposure with cytokine production (**Figure 1A, 1B**), as might be anticipated in settings of macrophage sensing of 'cell intrinsic' infection. Our results agree with published observations that SARS-CoV-2 does not trigger cytokine production from HMDM (*22*), and that SARS-CoV-2 also fails to trigger the interferon system in human alveolar macrophages (*21*). Findings from us and others (*21*, *22*) are, however, at odds with other reports that SARS-CoV-2 selectively induces a pro-inflammatory response (e.g., TNF, IL-6, CXCL10) from HMDM (*8*, *9*, *20*). It is possible that differences in the preparation or quantification of viral stocks may underpin these divergent observations. SARS-CoV-2 is usually cultured in cell lines (e.g., VERO E6 cells; Calu3 cells: (*8*)) that inherently respond to infection by producing cytokines or undergoing cell death. Indeed, virus is often harvested at a time point when a visible cytopathic effect emerges, meaning that individual viral preparations quantified for intact virions by $TCID_{50}$ or plaque assays may additionally contain free viral RNA, viral proteins, non-infectious virions, and parental cell line-derived DAMPs and cytokines (*37*). It is thus conceivable that published macrophage responses to viral preparations may represent an indirect response to epithelial infection or viral PAMPs. As such, selective macrophage pro-inflammatory responses that have been mapped to myeloid-expressed CLRs detecting glycosylated SARS-CoV-2 S (*23*), or cell surface TLR2 detecting viral envelope (E) protein (*26*) may reflect sensing of free viral proteins, rather than intact, infectious virions. Nevertheless, our viral stocks did not trigger cytokine release from human primary macrophages or THP-1 cells, unless ACE2 was ectopically expressed to allow SARS-CoV-2 entry and early-stage replication (**Figure 1A, 1B, Figure 5A**). This suggests that human macrophages do not sense infectious SARS-CoV-2 virions unless they are instructed to upregulate ACE2 expression. We anticipate that this observation will hold true for ACE2-

dependent SARS-CoV-2 variants, including Omicron (B.1.1.529 and BA lineages), and indeed any beta-coronaviruses that utilize ACE2. Consistent with this, SARS-CoV, which also requires ACE2 for entry, does not trigger macrophage cytokine responses (*38*).

We also observe that SARS-CoV-2 does not replicate in human macrophages and does not trigger productive virion release. This is in line with multiple reports of abortive SARS-CoV-2 infection of macrophages *in vitro* (*8*, *9*, *20*, *21*). While these studies observe that macrophage infection results in decreasing viral RNA levels (*8*, *9*, *20*), lack of new infectious virus (*8*, *20*), and decreasing viral protein (*21*), they nevertheless report virus entry into macrophages via quantification of SARS-CoV-2 nucleoprotein-positive cells. This is in contrast to studies reporting no infection of macrophages (*3*, *22*). We find that SARS-CoV-2 virions can enter macrophages, based on virion detection in phagosomes (**Figure 4A'**). Despite this entry into intracellular compartments, we propose that virus does not enter the macrophage cytoplasm, likely because ACE2 is required for conformational changes to the virus Spike protein that are necessary for viral membrane fusion. This may explain why viral RNA is detected within both airway-resident and recruited during single-cell RNA sequencing of BAL fluid from patients with severe COVID-19, despite low ACE2 expression in these cells (*4*, *23*, *39*).

Cellular ACE2 expression is dynamically regulated by factors such as interferons, and environmental cues within tissues, such as hypoxia (*40*). While we (this study) and others (*23*) find that resting primary human macrophages do not express ACE2 (**Figure 3A, 3B, 3C**), it is conceivable that *in vitro* culture or *in vivo* tissue conditions might induce macrophage ACE2 expression, which explain a report of macrophage ACE2 expression (*20*). Ectopic ACE2 expression in other cells that do not usually express ACE2, such as endothelial cells, renders these cells susceptible and permissive to productive SARS-CoV-2 infection (*28*). In THP-1 cells, ACE2 overexpression indeed facilitated SARS-CoV-2 entry and early-stage replication, but in response, these cells initiated an interferon program to prevent productive infection (**Figure 3F, 3G, 5A, 6D**). This mechanism appeared to block virion production at a stage beyond genome replication (as measured by viral RNA, **Figures 3D-E**), perhaps during virion assembly or release. Thus, even if macrophages do induce ACE2 expression during virus encounter, they are unlikely to act as 'trojan horses' to disseminate SARS-CoV-2 to extra-respiratory tissues. This is consistent with abortive replication of other respiratory viruses in human macrophages, including seasonal influenza A virus (*41*) and

rhinovirus (*15*).The molecular mechanisms underpinning why macrophages are resistant to productive respiratory virus infection, remain to be elucidated.

Macrophages are key sentinels for microbial infection and can usually detect pathogen-derived molecules with exquisite sensitivity. Our data indicates that SARS-CoV-2 evades detection by human macrophages. It is tempting to speculate that the severe disease caused by SARS-CoV-2 may partially derive from its capacity to evade macrophage detection and resultant anti-viral responses. Macrophage-derived interferon is critical for controlling other respiratory viral infections (e.g. Newcastle Disease Virus, Respiratory Syncytial Virus) (*17*, *18*), and here, cytosolic viral sensors such as retinoic acid-inducible gene-1 (RIG-I) and MDA5 induce robust interferon responses to rapidly control viral replication. In contrast, viruses that do not infect macrophages, such as SARS-CoV-2, may be able to persist and replicate for longer in the absence of a macrophage interferon response, causing ongoing epithelial and other cell damage, which may perpetuate inflammation and immunopathology. In the inflamed, SARS-CoV-2-infected lung, we expect that macrophages will sense cell 'extrinsic' danger by sampling the extracellular space and phagosomal compartments (*42*). In this scenario, macrophage cell surface (e.g., CLRs, TLR2 (*23*, *26*)) or endosomal PRRs (e.g. TLR7/8) could sense such cell-extrinsic signals to preferentially activate pro-inflammatory signalling instead of anti-viral interferons (*43*), contributing to disease.

Our study indicates that SARS-CoV-2 is not sensed by human macrophages unless ACE2 expression is induced, and early-stage viral replication can occur. This study gives new insight into SARS-CoV-2 cell tropism, and the influence therein of macrophage innate immune pathways. Such studies of innate immune cell-intrinsic and -extrinsic SARS-CoV-2 recognition and response will help reveal novel therapeutic targets for new drugs that dampen pathogenic pro-inflammatory signalling in virulent viral infections, without impeding host anti-viral defence.

MATERIALS AND METHODS

Reagents and inhibitors

Low molecular weight Poly I:C (Invivogen, tlrl-picw) was transfected into cells with lipofectamine LTX (Thermofisther, A12621) at 0.5 μg pIC per well, while R848 Resiquimod

(Miltenyi Biotech, 130-109-376) was used at a final concentration of 250 ng/ml. The TBK1 inhibitor BX-795 (Sigma-Aldrich, SML0694) was used at a final concentration of 5 μM.

Cells

Peripheral blood mononuclear cells were isolated from buffy coats by density centrifugation using Ficoll-Paque Plus (GE Healthcare). CD14+ monocytes were subsequently isolated using magnetic-activated cell sorting (Miltenyi Biotech), according to the manufacturer's instructions. Human macrophages were differentiated from human CD14+ monocytes as previously described (*44*) and then used for experiments on day 7 of differentiation. Human monocyte-derived macrophages (HMDMs) were cultured in media consisting of RPMI 1640 medium (Life Technologies) supplemented with 10% heat-inactivated fetal bovine serum (FBS), 2mM GlutaMAX (Life Technologies), 50 U/ml penicillin–streptomycin (Life Technologies) and 150 ng/ml recombinant human macrophage colony-stimulating factor (CSF-1, endotoxin free, expressed and purified by the University of Queensland Protein Expression Facility). HMDM were seeded 16 h prior to experiments at 500 000 cells per well in 12 well plates, or 200 000 cells per well in 24 well plates. Studies using primary human cells were approved by the University of Queensland Human Medical Research Ethics Committee. THP-1 cells (TIB-202; ATCC) were maintained in RPMI 1640 medium supplemented with 10% heat-inactivated foetal bovine serum (FBS), 2 mM GlutaMAX (Life Technologies) and 50 U/ml penicillin–streptomycin (Life Technologies). For experiments, THP-1 cells were seeded at 500 000 cells per well of a 12-well plate and differentiated for 48 h with 30 ng/ml phorbol-myristate-acetate (PMA). Calu-3 cells purchased from ATCC (HTB-55) were maintained in Minimal Essential Media (Invitrogen), containing 10% heat-inactivated foetal bovine serum (Cytiva), 50 U/ml penicillin and streptomycin (Life Technologies Australia), and were seeded at 300 000 cells per well in a 12-well plate 48 h prior to experiments.

Patient bronchoalveolar lavage (BAL) was obtained at the time of diagnostic bronchoscopy as previously described (*45*). Briefly, the bronchoscope was wedged into a non-dependent sub-segmental bronchus (*46*) of a radiologically normal segment of lung, and 20 ml of normal saline was instilled, retrieved, and discarded to clear the bronchoscope of bronchial secretions. A further 80-100 ml was instilled in 20-ml aliquots and retrieved via hand aspiration of the syringe. Studies using primary human cells were approved by the Royal

Melbourne Hospital and University of Melbourne Human Research Ethics Committees. BAL was filtered and cells washed and seeded at $1x10^6$ cells per ml, overnight, in 48 well tissue culture plates in RPMI 1640 medium supplemented with 10% heat-inactivated foetal bovine serum (FBS), 2 mM GlutaMAX (Life Technologies) and 50 U/ml penicillin–streptomycin (Life Technologies). Non-adherent cells were removed via media change four hours post-seeding, resulting in >90% macrophage population, as described previously (*47*).

Lentiviral transduction

A lentiviral construct containing human ACE2 (Addgene 155295), or mScarlet (Addgene 85044) was cloned into pLV-CMV-MCS-IRES-Puro-Sin (*48*) and packaged into lentivirus in HEK-293T cells by means of third generation lentiviral packaging plasmids (*49*). Lentivirus-containing supernatant was harvested on day 2 and 3 after transfection. Lentivirus was concentrated by Lenti-X concentrator (Clontech, 631232). HEK-293T cells were transfected with the expression vectors according to the manufacturer's protocol with PEI 2500 (BioScientific) and transduced target THP-1 cells were selected with puromycin (1 μg/mL) after 24 h and used for assays after 72 h.

Viruses and cell infections

SARS-CoV-2 isolate hCoV-19/Australia/QLD02/2020 was provided by Queensland Health Forensic & Scientific Services, Queensland Department of Health. Virus was grown on Vero E6 TMPRSS2 cells for 48 h in DMEM with 2% FBS, and cell debris was cleared by centrifugation at 500G for 5 minutes at room temperature. Virus was titred as described previously by plaque assay (*28*). Sanger sequencing was used to confirm that no mutations occurred in the spike gene relative to the original clinical isolate. Cells (HMDM, THP-1, Calu3) in 12 well plates (500 000 cells/well) were challenged for 1 h at 37°C and 5% CO_2 with 2.5 x 10^6 plaque-forming units (PFUs) for MOI 5, or 2.5 x 10^5 PFUs for MOI 0.5. For Calu3 cells, virus was added to cells to give a total volume of 500 μL of RPMI 1640 with 2% FBS (HMDM and THP-1) or MEM with 2% FBS (Calu3) per well. The viral inoculum was then removed, and the medium was replaced with DMEM (Invitrogen) or MEM (Invitrogen) containing 2% FBS. Alternatively, virus was not removed from the cells. All studies with SARS-CoV-2 were performed under physical containment 3 (PC3) conditions and were approved by The University of Queensland Biosafety Committee (IBC/374B/ SCMB/2020, IBC/518B/IMB/SCMB/2022) and the University of Melbourne Institutional Biosafety

Committee in consultation with the Doherty Institute High Containment Facility Management Group.

For studies involving SARS-CoV-2 infection of BAL macrophages**,** the SARS-CoV-2 isolate hCoV-19/Australia/VIC01/2020 (kindly provided by the Victorian Infectious Diseases Reference Laboratory) was grown in Vero cells for 72 h in serum-free MEM with 1 μg/ml TPCK trypsin. The median tissue culture infectious dose ($TCID_{50}$) was calculated using the Reed-Muench method. BAL macrophages (approx. 2.5 x 10^5 cells) were seeded overnight in 48 well plates. Macrophages were infected with SARS-CoV-2 (MOI 1) in serum free media (RPMI supplemented as described above) for 1 hr. Inoculum was removed and cells were washed, before media was replaced 400 μL serum free media for a further 2 to 48 hrs. VERO control cells were infected at an MOI of 0.5 and maintenance media included 1μg/ml of TPCK trypsin. RNA from cell free supernatant was collected and extracted using QIAamp Viral RNA Mini Kit (Qiagen) while RNA from cell monolayers was extracted via the Rneasy Plus Mini Kit (Qiagen).

Cell Death

THP-1 were seeded at 50 000 cells per well of a black walled clear bottomed 96 well plate (CLS3916, Corning). After 48h of differentiation with PMA, cells were inoculated with virus at MOI 5, incubated for 1h, before media was replaced with 100 μl of fresh RPMI with 2% FCS. After 72h, ~60 μl of media was removed per well, leaving 30 μl and 30 μl of ATPlite substrate solution (Perkin Elmer) was added per well. After 10 minutes incubation at room temperature, plates were sealed with Optical Adhesive Film (Thermofisher) and luminescence was read on a Victor Nivo Plate Reader (Perkin Elmer).

RNA extraction and qPCR analysis

Cells were lysed in Buffer RLT plus β-mercaptoethanol, and RNA was directly processed using the Rneasy Mini Kit (Qiagen), with on-column Dnase digestion according to manufacturer's instructions. RNA concentration was measured using a NanoDrop spectrophotometer and an equal starting concentration of RNA for each sample was used for reverse transcription. Reverse transcription was performed using Superscript III Reverse Transcriptase (ThermoFisher) with random hexamer priming. Quantitative PCR was performed using SYBR green reagent (Applied Biosystems) on a QuantStudio 7 Flex Real-

Time PCR System (ThermoFisher) in 384 well plates (Applied Biosystems) and relative gene expression was determined using the change-in-threshold ($2^{-\Delta\Delta CT}$) method, using Hypoxanthine Phosphoribosyltransferase 1 (*Hprt*) as an endogenous control. Alternatively, gene expression was determined relative to a standard curve generated from plasmids containing SARS-CoV-2 Main Protease (Mpro). Primers are as follows: *Hprt* F*:* TCAGGCAGTATAATCCAAAGATGGT R: AGTCTGGCTTATATCCAACACTTCG; *Ace2* F: TCACGATTGTTGGGACTCTGC, R: TCGCTTCATCTCCCACCACT; *Il6* F: CTCAGCCCTGAGAAAGGAGACAT, R: TCAGCCATCTTTGGAAGGTTCA; *Tnf* F: TGCCTGCTGCACTTTGGAGTGA, R: AGATGATCTGACTGCCTGGGCCAG; *Il1b* F: GAAGCTGATGGCCCTAAACA, R: AAGCCCTTGCTGTAGTGGTG, *Ifnb1* F: CAGTCCTGGAAGAAAAACTGGAGA, R: TTGGCCTTCAGGTAATGCAGAA; *Cxcl10* F: TGAAAGCAGTTAGCAAGGAAAGGT, R: AGCCTCTGTGTGGTCCATCC; *Ifnl1* F: CGCCTTGGAAGAGTCACTCA, R: GAAGCCTCAGGTCCCAATTC; SARS-CoV-2 *Mpro* F: GAGACAGGTGGTTTCTCAATCG, R: ACGGCAATTCCAGTTTGAGC; SARS-CoV-2 *E* gene F: ACAGGTACGTTAATAGTTAATAGCGT, R: ATATTGCAGCAGTACGCACACA.

Copy number of SARS-CoV-2 E gene was measured in cellular RNA (equal starting concentration of RNA) and RNA from cell culture media (equal starting volume). SensiFAST™ Probe Lo-ROX One-Step Kit with E-specific probe (FAM-ACACTAGCCATCCTTACTGCGCTTCG-QQA) was used to detect E gene and a plasmid-based standard curves was used to quantify the number of E copies. The Mpro sequence was amplified from cDNA with the Phusion polymerase kit (New England BioLabs) using the following primers. F: AATAAGGTACCAGTGGTTTTAGAAAAATGG, R: TTATTGCGGCCGCTCATTGGAAAGTAACACC. The Mpro expression vector was generated by cloning the Mpro PCR product into a modified pEF6 plasmid, with an HA-tag N-terminal of the multiple cloning site, by standard restriction digest cloning techniques. The vector and correct insertion of Mpro were verified by Sanger sequencing.

Cytokine analysis

Cytokine titres were determined using an AlphaLISA Immunoassay kit (Perkin Elmer) according to the manufacturer's instructions and analysed on a Victor Nivo Plate Reader (Perkin Elmer).

Electron Microscopy

Electron Microscopy samples were processed using a method adapted from a previous study (*50*). Briefly cells were fixed in 2.5% glutaraldehyde (Electron Microscopy Services) in PBS for 24 h, then post fixed in 1% osmium (ProSciTech) for 1 h and contrasted with 1% aqueous uranyl acetate (Electron Microscopy Services) for 1 h. Samples were then serially dehydrated in increasing percentages of ethanol before serial infiltration with LX-112 resin (Ladd Research) in a Biowave microwave (Pelco). Ultrathin sections were attained on a ultramicrotome (UC6:Leica), and further contrasted using Reynold lead post-stain. Micrographs were acquired using a JEOL 1011 transmission microscope at 80 kV with a Morada CCD camera (Olympus) utilising iTEM software.

Immunoblotting

For total cell lysates, cells were washed once with PBS and lysed with RIPA buffer (50 mM Tris, 150 mM NaCl, 1 mM EDTA, 1% Triton X-100, 0.1% SDS, 1% sodium deoxycholate, protease inhibitor, pH 8.0). A Pierce BCA protein assay kit (Thermo Scientific) was used to equalise protein amounts. SDS sample buffer containing 100 mM DTT (Astral Scientific) was added, and samples were boiled at 95°C for 10 min to denature proteins. Proteins were separated on 4-15% mini protean TGX precast gels (Bio-Rad) in running buffer (200 mM Glycine, 25 mM Tris, 0.1% SDS (pH8.6)), transferred to PVDF or nitrocellulose membrane (Bio-Rad 1620112) in blot buffer (48 nM Tris, 39 nM Glycine, 0.04% SDS, 20% MeOH) and subsequently blocked with 5% (w/v) milk powder or BSA in Tris-buffered saline with Tween-20 (TBST) for 30 min. Primary antibodies were incubated overnight at 4 deg C, followed by secondary antibodies linked to horseradish peroxidase (HRP) (Cell Signalling) or AlexaFluor647 (Invitrogen), and after each step, immunoblots were washed 3x with TBST. HRP signals were visualised by enhanced chemiluminescence (ECL) (Bio-Rad) and imaged with a Vilber Fusion Imaging system (Vilber). Fluorescence signal was detected using the AI600 imager (Amersham). The following antibodies were used: SARS-CoV-2 Nucleoprotein (Sino Biological), Tubulin (9F3; Cell Signalling Technology), ACE2 (AF933; RnD Systems), TMPRSS2 (Abcam) and Actin (8H10D10; Cell Signalling Technology), ACE2 (MA532307, Invitrogen), Calnexin (ab22595, Abcam).

Statistical Analysis:

Statistics were calculated using GraphPad Prism using tests indicated in figure legends.

Supplementary Materials

Figure S1: Macrophage ACE2 expression potentiates macrophage inflammatory responses to SARS-CoV-2 at MOI 0.5 (Relates to Figure 5).

Figure S2: BX-795 blocks anti-viral cytokine induction in THP1-ACE2 cells (Relates to Figure 6).

ACKNOWLEDGEMENTS

We gratefully acknowledge Dr Emma Gordon and Dr Lilian Schimmel for production of the ACE2 and mScarlet expressing lentiviruses and Dr Fiona Wylie for critical reading of this manuscript. This work was supported by National Health and Medical Research Council (NHMRC) of Australia funding including fellowships (1124612 to LL; 1177174 to K. Subbaro; 1156489 to RGP; 2009075 to K. Schroder) and grants (1140064 and 1150083 to RGP; 2007979 to KRS; 1184532 to SL; 2009677 to K. Schroder) and the Doherty Institute COVID-19 Agility Fund. The Melbourne WHO Collaborating Centre for Reference and Research on Influenza is supported by the Australian Government Department of Health.

COMPETING INTERESTS:

KRS is a consultant for Sanofi, Roche and NovoNordisk. K. Schroder is a co-inventor on patent applications for NLRP3 inhibitors which have been licensed to Inflazome Ltd, a company headquartered in Dublin, Ireland. Inflazome is developing drugs that target the NLRP3 inflammasome to address unmet clinical needs in inflammatory disease. K. Schroder served on the Scientific Advisory Board of Inflazome in 2016–2017, and serves as a consultant to Quench Bio, USA and Novartis, Switzerland.

AUTHOR CONTRIBUTIONS

Conception: LIL and SLL

Data acquisition and Analysis: LIL, KYC, XW, TE, CJS, JR, TY, CLH, SE, SF, FLM, DPS, AKL, RGP, SLL

Funding acquisition: LIL, SLL, K.Schroder

Manuscript original draft: LIL, K.Schroder

Manuscript editing: LIL, K.Subbarao, KRS, SLL, K.Schroder

REFERENCES

1. Y. J. Hou, K. Okuda, C. E. Edwards, D. R. Martinez, K. H. Dinnon, T. Kato, R. E. Lee, B. L. Yount, T. M. Mascenik, G. Chen, K. N. Olivier, A. Ghio, V. Longping, S. R. Leist, L. E. Gralinski, A. Schäfer, H. Dang, S. Nakano, L. Sun, M. L. Fulcher, A. Livraghi-butrico, N. I. Nicely, M. Cameron, C. Cameron, D. J. Kelvin, A. De, D. M. Margolis, A. Markmann, L. Bartelt, R. Zumwalt, J. Martinez, S. P. Salvatore, A. Borczuk, P. R. Tata, A. Kimple, I. Jaspers, W. K. O. Neal, S. H. Randell, C. Richard, R. S. Baric, SARS-CoV-2 Reverse Genetics Reveals a Variable Infection Gradient in the Respiratory Tract. *Cell* (2020), doi:10.1016/j.cell.2020.05.042.
2. D. Blanco-Melo, B. E. Nilsson-Payant, W.-C. Liu, S. Uhl, D. Hoagland, R. Møller, T. X. Jordan, K. Oishi, M. Panis, D. Sachs, T. T. Wang, R. E. Schwartz, J. K. Lim, R. A. Albrecht, B. R. Tenoever, Imbalanced host response to SARS-CoV-2 drives development of COVID-19. *Cell*, 1–10 (2020).
3. L. G. Thorne, A. Reuschl, L. Zuliani-Alvarez, M. V. X. Whelan, J. Turner, M. Noursadeghi, C. Jolly, G. J. Towers, SARS-CoV-2 sensing by RIG-I and MDA5 links epithelial infection to macrophage inflammation. *EMBO J.*, 1–17 (2021).
4. P. Bost, A. Giladi, Y. Liu, Y. Bendjelal, G. Xu, E. David, R. Blecher-Gonen, M. Cohen, C. Medaglia, H. Li, A. Deczkowska, S. Zhang, B. Schwikowski, Z. Zhang, I. Amit, Host-viral infection maps reveal signatures of severe COVID-19 patients. *Cell* (2020), doi:10.1016/j.cell.2020.05.006.
5. R. L. Chua, S. Lukassen, S. Trump, B. P. Hennig, D. Wendisch, F. Pott, O. Debnath, L. Thürmann, F. Kurth, M. T. Völker, J. Kazmierski, B. Timmermann, S. Twardziok, S. Schneider, F. Machleidt, H. Müller-Redetzky, M. Maier, A. Krannich, S. Schmidt, F. Balzer, J. Liebig, J. Loske, N. Suttorp, J. Eils, N. Ishaque, U. G. Liebert, C. von Kalle, A. Hocke, M. Witzenrath, C. Goffinet, C. Drosten, S. Laudi, I. Lehmann, C. Conrad, L. E. Sander, R. Eils, COVID-19 severity correlates with airway epithelium–immune cell interactions identified by single-cell analysis. *Nat. Biotechnol.* **38**, 970–979 (2020).
6. R. Knoll, J. L. Schultze, J. Schulte-Schrepping, Monocytes and Macrophages in COVID-19. *Front. Immunol.* **12**, 1–12 (2021).
7. M. Merad, J. C. Martin, Pathological inflammation in patients with COVID-19: a key role for monocytes and macrophages. *Nat. Rev. Immunol.* **20**, 355–362 (2020).
8. J. Zheng, Y. Wang, K. Li, D. K. Meyerholz, C. Allamargot, S. Perlman, Severe Acute Respiratory Syndrome Coronavirus 2-Induced Immune Activation and Death of Monocyte-Derived Human Macrophages and Dendritic Cells. *J. Infect. Dis.* **223**, 785–795 (2021).
9. D. Yang, H. Chu, Y. Hou, Y. Chai, H. Shuai, A. C. Y. Lee, X. Zhang, Y. Wang, B. Hu, X. Huang, T. T. T. Yuen, J. P. Cai, J. Zhou, S. Yuan, A. J. Zhang, J. F. W. Chan, K. Y. Yuen, Attenuated interferon and proinflammatory response in SARS-CoV-2-infected human dendritic cells is associated with viral antagonism of STAT1 phosphorylation. *J. Infect. Dis.* **222**, 734–745 (2020).
10. M. Hoffmann, H. Kleine-Weber, S. Schroeder, M. A. Mü, C. Drosten, S. Pö, N. Krü, T. Herrler, S. Erichsen, T. S. Schiergens, G. Herrler, N.-H. Wu, A. Nitsche, S. Pö Hlmann, SARS-CoV-2 Cell Entry Depends on ACE2 and TMPRSS2 and Is Blocked by a Clinically Proven Protease Inhibitor Article SARS-CoV-2 Cell Entry Depends on ACE2 and TMPRSS2 and Is Blocked by a Clinically Proven Protease Inhibitor. *Cell.* **181**, 1–10 (2020).
11. C. B. Jackson, M. Farzan, B. Chen, H. Choe, Mechanisms of SARS-CoV-2 entry into cells. *Nat. Rev. Mol. Cell Biol.* **0123456789** (2021), doi:10.1038/s41580-021-00418-x.

12. P. V'kovski, A. Kratzel, S. Steiner, H. Stalder, V. Thiel, Coronavirus biology and replication: implications for SARS-CoV-2. *Nat. Rev. Microbiol.* **19**, 155–170 (2021).
13. B. Meng, A. Abdullahi, I. A. T. M. Ferreira, N. Goonawardane, A. Saito, I. Kimura, D. Yamasoba, P. P. Gerber, S. Fatihi, S. Rathore, S. K. Zepeda, G. Papa, S. A. Kemp, T. Ikeda, M. Toyoda, T. S. Tan, J. Kuramochi, S. Mitsunaga, T. Ueno, K. Shirakawa, A. Takaori-Kondo, T. Brevini, D. L. Mallery, O. J. Charles, CITIID-NIHR BioResource COVID- Collaboration, Genotype to Phenotype Japan (GP-Japan) Consortium members, Ecuador-COVID19 Consortium, J. E. Bowen, A. Joshi, A. C. Walls, L. Jackson, D. Martin, K. G. C. Smith, J. Bradley, J. A. G. Briggs, J. Choi, E. Madissoon, K. Meyer, P. Mlcochova, L. Ceron-Gutierrez, R. Doffinger, S. A. Teichmann, A. J. Fisher, M. S. Pizzuto, A. de Marco, D. Corti, M. Hosmillo, J. H. Lee, L. C. James, L. Thukral, D. Veesler, A. Sigal, F. Sampaziotis, I. G. Goodfellow, N. J. Matheson, K. Sato, R. K. Gupta, Altered TMPRSS2 usage by SARS-CoV-2 Omicron impacts tropism and fusogenicity. *Nature* (2022), doi:10.1038/s41586-022-04474-x.
14. K. R. Short, A. G. Brooks, P. C. Reading, S. L. Londrigan, The fate of influenza A virus after infection of human macrophages and dendritic cells. *J. Gen. Virol.* **93**, 2315–2325 (2012).
15. J. E. Gern, E. C. Dick, W. M. Lee, S. Murray, K. Meyer, Z. T. Handzel, W. W. Busse, Rhinovirus enters but does not replicate inside monocytes and airway macrophages. *J. Immunol.* **156**, 621–7 (1996).
16. S. L. Londrigan, L. M. Wakim, J. Smith, A. J. Haverkate, A. G. Brooks, P. C. Reading, IFITM3 and type I interferons are important for the control of influenza A virus replication in murine macrophages. *Virology*. **540**, 17–22 (2020).
17. M. Goritzka, S. Makris, F. Kausar, L. R. Durant, C. Pereira, Y. Kumagai, F. J. Culley, M. Mack, S. Akira, C. Johansson, Alveolar macrophage-derived type I interferons orchestrate innate immunity to RSV through recruitment of antiviral monocytes. *J. Exp. Med.* **212**, 699–714 (2015).
18. Y. Kumagai, O. Takeuchi, H. Kato, H. Kumar, K. Matsui, E. Morii, K. Aozasa, T. Kawai, S. Akira, Alveolar Macrophages Are the Primary Interferon-α Producer in Pulmonary Infection with RNA Viruses. *Immunity*. **27**, 240–252 (2007).
19. C. Schneider, S. P. Nobs, A. K. Heer, M. Kurrer, G. Klinke, N. van Rooijen, J. Vogel, M. Kopf, Alveolar Macrophages Are Essential for Protection from Respiratory Failure and Associated Morbidity following Influenza Virus Infection. *PLoS Pathog.* **10** (2014), doi:10.1371/journal.ppat.1004053.
20. M. M. Abdelmoaty, P. Yeapuri, J. Machhi, K. E. Olson, F. Shahjin, V. Kumar, Y. Zhou, J. Liang, K. Pandey, A. Acharya, S. N. Byrareddy, R. L. Mosley, H. E. Gendelman, Defining the Innate Immune Responses for SARS-CoV-2-Human Macrophage Interactions. *Front. Immunol.* **12**, 1–15 (2021).
21. L. Dalskov, M. Møhlenberg, J. Thyrsted, J. Blay-Cadanet, E. T. Poulsen, B. H. Folkersen, S. H. Skaarup, D. Olagnier, L. Reinert, J. J. Enghild, H. J. Hoffmann, C. K. Holm, R. Hartmann, SARS-CoV-2 evades immune detection in alveolar macrophages. *EMBO Rep.* **21**, 1–10 (2020).
22. M. A. Niles, P. Gogesch, S. Kronhart, S. Ortega Iannazzo, G. Kochs, Z. Waibler, M. Anzaghe, Macrophages and Dendritic Cells Are Not the Major Source of Pro-Inflammatory Cytokines Upon SARS-CoV-2 Infection. *Front. Immunol.* **12**, 1–12 (2021).
23. Q. Lu, J. Liu, S. Zhao, M. F. Gomez Castro, M. Laurent-Rolle, J. Dong, X. Ran, P. Damani-Yokota, H. Tang, T. Karakousi, J. Son, M. E. Kaczmarek, Z. Zhang, S. T. Yeung, B. T. McCune, R. E. Chen, F. Tang, X. Ren, X. Chen, J. C. C. Hsu, M. Teplova, B. Huang, H. Deng, Z. Long, T. Mudianto, S. Jin, P. Lin, J. Du, R. Zang, T.

T. Su, A. Herrera, M. Zhou, R. Yan, J. Cui, J. Zhu, Q. Zhou, T. Wang, J. Ma, S. B. Koralov, Z. Zhang, I. Aifantis, L. N. Segal, M. S. Diamond, K. M. Khanna, K. A. Stapleford, P. Cresswell, Y. Liu, S. Ding, Q. Xie, J. Wang, SARS-CoV-2 exacerbates proinflammatory responses in myeloid cells through C-type lectin receptors and Tweety family member 2. *Immunity*. **54**, 1304-1319.e9 (2021).

24. C. Lucas, P. Wong, J. Klein, T. B. R. Castro, J. Silva, M. Sundaram, M. K. Ellingson, T. Mao, J. E. Oh, B. Israelow, T. Takahashi, M. Tokuyama, P. Lu, A. Venkataraman, A. Park, S. Mohanty, H. Wang, A. L. Wyllie, C. B. F. Vogels, R. Earnest, S. Lapidus, I. M. Ott, A. J. Moore, M. C. Muenker, J. B. Fournier, M. Campbell, C. D. Odio, A. Casanovas-Massana, A. Obaid, A. Lu-Culligan, A. Nelson, A. Brito, A. Nunez, A. Martin, A. Watkins, B. Geng, C. Kalinich, C. Harden, C. Todeasa, C. Jensen, D. Kim, D. McDonald, D. Shepard, E. Courchaine, E. B. White, E. Song, E. Silva, E. Kudo, G. DeIuliis, H. Rahming, H. J. Park, I. Matos, J. Nouws, J. Valdez, J. Fauver, J. Lim, K. A. Rose, K. Anastasio, K. Brower, L. Glick, L. Sharma, L. Sewanan, L. Knaggs, M. Minasyan, M. Batsu, M. Petrone, M. Kuang, M. Nakahata, M. Campbell, M. Linehan, M. H. Askenase, M. Simonov, M. Smolgovsky, N. Sonnert, N. Naushad, P. Vijayakumar, R. Martinello, R. Datta, R. Handoko, S. Bermejo, S. Prophet, S. Bickerton, S. Velazquez, T. Alpert, T. Rice, W. Khoury-Hanold, X. Peng, Y. Yang, Y. Cao, Y. Strong, R. Herbst, A. C. Shaw, R. Medzhitov, W. L. Schulz, N. D. Grubaugh, C. Dela Cruz, S. Farhadian, A. I. Ko, S. B. Omer, A. Iwasaki, Longitudinal analyses reveal immunological misfiring in severe COVID-19. *Nature*. **584**, 463–469 (2020).

25. M. Koutsakos, L. C. Rowntree, L. Hensen, B. Y. Chua, C. E. van de Sandt, J. R. Habel, W. Zhang, X. Jia, L. Kedzierski, T. M. Ashhurst, G. H. Putri, F. Marsh-Wakefield, M. N. Read, D. N. Edwards, E. B. Clemens, C. Y. Wong, F. L. Mordant, J. A. Juno, F. Amanat, J. Audsley, N. E. Holmes, C. L. Gordon, O. C. Smibert, J. A. Trubiano, C. M. Hughes, M. Catton, J. T. Denholm, S. Y. Tong, D. L. Doolan, T. C. Kotsimbos, D. C. Jackson, F. Krammer, D. I. Godfrey, A. W. Chung, N. J. King, S. R. Lewin, A. K. Wheatley, S. J. Kent, K. Subbarao, J. McMahon, I. Thevarajan, T. H. Nguyen, A. C. Cheng, K. Kedzierska, Integrated immune dynamics define correlates of COVID-19 severity and antibody responses. *Cell Reports Med.*, 100208 (2021).

26. M. Zheng, R. Karki, E. P. Williams, D. Yang, E. Fitzpatrick, P. Vogel, C. B. Jonsson, T. D. Kanneganti, TLR2 senses the SARS-CoV-2 envelope protein to produce inflammatory cytokines. *Nat. Immunol.* **22**, 829–838 (2021).

27. C. Blériot, S. Chakarov, F. Ginhoux, Determinants of Resident Tissue Macrophage Identity and Function. *Immunity*. **52**, 957–970 (2020).

28. L. Schimmel, K. Y. Chew, C. J. Stocks, T. E. Yordanov, P. Essebier, A. Kulasinghe, J. Monkman, A. F. R. Santos Miggiolaro, C. Cooper, L. Noronha, K. Schroder, A. K. Lagendijk, L. I. Labzin, K. R. Short, E. J. Gordon, Endothelial cells are not productively infected by SARS-CoV-2. *Clin. Transl. Immunol.* **10**, 1–18 (2021).

29. L. I. Labzin, M. Bottermann, P. Rodriguez-Silvestre, S. Foss, J. T. Andersen, M. Vaysburd, D. Clift, L. C. James, Antibody and DNA sensing pathways converge to activate the inflammasome during primary human macrophage infection. *EMBO J.* **38**, e101365 (2019).

30. S. S. Diebold, T. Kaisho, H. Hemmi, S. Akira, C. Reis E Sousa, Innate Antiviral Responses by Means of TLR7-Mediated Recognition of Single-Stranded RNA. *Science (80-.).* **303**, 1529–1531 (2004).

31. M. Weber, A. Gawanbacht, M. Habjan, A. Rang, C. Borner, A. M. Schmidt, S. Veitinger, R. Jacob, S. Devignot, G. Kochs, A. García-Sastre, F. Weber, Incoming RNA virus nucleocapsids containing a 5′-triphosphorylated genome activate RIG-I and antiviral signaling. *Cell Host Microbe*. **13**, 336–346 (2013).

32. C. Junqueira, Â. Crespo, S. Ranjbar, J. Ingber, B. Parry, S. Ravid, L. B. de Lacerda, M. Lewandrowski, S. Clark, F. Ho, S. M. Vora, V. Leger, C. Beakes, J. Margolin, N. Russell, L. Gehrke, U. Das Adhikari, L. Henderson, E. Janssen, D. Kwon, C. Sander, J. Abraham, M. Filbin, M. B. Goldberg, H. Wu, G. Mehta, S. Bell, A. E. Goldfeld, J. Lieberman, SARS-CoV-2 infects blood monocytes to activate NLRP3 and AIM2 inflammasomes, pyroptosis and cytokine release. *medRxiv Prepr. Serv. Heal. Sci.* (2021), doi:10.1101/2021.03.06.21252796.

33. J. W. Schoggins, Interferon-stimulated genes: Roles in viral pathogenesis. *Curr. Opin. Virol.* **6**, 40–46 (2014).

34. K. Clark, L. Plater, M. Peggie, P. Cohen, Use of the pharmacological inhibitor BX795 to study the regulation and physiological roles of TBK1 and IκB Kinase ∈:A distinct upstream kinase mediates ser-172 phosphorylation and activation. *J. Biol. Chem.* **284**, 14136–14146 (2009).

35. K. M. Franz, J. C. Kagan, Innate Immune Receptors as Competitive Determinants of Cell Fate. *Mol. Cell.* **66**, 750–760 (2017).

36. A. Iwasaki, P. S. Pillai, Innate immunity to influenza virus infection. *Nat. Rev. Immunol.* **14**, 315–328 (2014).

37. Q. Niu, L. Ma, S. Zhu, L. Li, Q. Zheng, J. Hou, H. Lian, L. Wu, X. Yan, Quantitative Assessment of the Physical Virus Titer and Purity by Ultrasensitive Flow Virometry. *Angew. Chemie - Int. Ed.* **60**, 9351–9356 (2021).

38. O. García-Nicolás, P. V'kovski, F. Zettl, G. Zimmer, V. Thiel, A. Summerfield, No Evidence for Human Monocyte-Derived Macrophage Infection and Antibody-Mediated Enhancement of SARS-CoV-2 Infection. *Front. Cell. Infect. Microbiol.* **11**, 1–10 (2021).

39. R. A. Grant, L. Morales-Nebreda, N. S. Markov, S. Swaminathan, M. Querrey, E. R. Guzman, D. A. Abbott, H. K. Donnelly, A. Donayre, I. A. Goldberg, Z. M. Klug, N. Borkowski, Z. Lu, H. Kihshen, Y. Politanska, L. Sichizya, M. Kang, A. Shilatifard, C. Qi, J. W. Lomasney, A. C. Argento, J. M. Kruser, E. S. Malsin, C. O. Pickens, S. B. Smith, J. M. Walter, A. E. Pawlowski, D. Schneider, P. Nannapaneni, H. Abdala-Valencia, A. Bharat, C. J. Gottardi, G. R. S. Budinger, A. V. Misharin, B. D. Singer, R. G. Wunderink, R. A. Grant, L. Morales-Nebreda, N. S. Markov, S. Swaminathan, M. Querrey, E. R. Guzman, D. A. Abbott, H. K. Donnelly, A. Donayre, I. A. Goldberg, Z. M. Klug, N. Borkowski, Z. Lu, H. Kihshen, Y. Politanska, L. Sichizya, M. Kang, A. Shilatifard, C. Qi, J. W. Lomasney, A. C. Argento, J. M. Kruser, E. S. Malsin, C. O. Pickens, S. B. Smith, J. M. Walter, A. E. Pawlowski, D. Schneider, P. Nannapaneni, H. Abdala-Valencia, A. Bharat, C. J. Gottardi, G. R. S. Budinger, A. V. Misharin, B. D. Singer, R. G. Wunderink, A. A. Wagh, A. R. Hauser, A. R. Wolfe, A. Thakrar, A. V. Yeldandi, A. A. Wang, A. R. Levenson, A. M. Joudi, B. Tran, C. A. Gao, C. Kurihara, C. J. Schroedl, C. M. Horvath, D. Meza, D. D. Odell, D. W. Kamp, D. R. Winter, E. A. Ozer, E. D. Shanes, E. T. Bartom, E. J. Rendleman, E. M. Leibenguth, F. Wehbe, G. Y. Liu, G. T. Gadhvi, H. T. Navarro, J. I. Sznajder, J. E. Dematte, J. Le, J. M. Arnold, J. C. Du, J. Coleman, J. I. Bailey, J. S. Deters, J. A. Fiala, J. Starren, K. M. Ridge, K. Secunda, K. Aren, K. L. Gates, K. Todd, L. D. Gradone, L. N. Textor, L. F. Wolfe, L. L. Pesce, L. A. Nunes Amaral, M. L. Rosenbaum, M. Kandpal, M. Jain, M. A. Sala, M. Saine, M. Carns, M. J. Alexander, M. J. Cuttica, M. H. Prickett, N. H. Khan, N. S. Chandel, N. D. Soulakis, O. R. Rivas, P. C. Seed, P. A. Reyfman, P. D. Go, P. H. S. Sporn, P. R. Cooper, R. Tomic, R. Patel, R. Garza-Castillon, R. Kalhan, R. I. Morimoto, R. J. Mylvaganam, S. S. Kim, S. W. M. Gatesy, S. Thakkar, S. Ben Maamar, S. H. Han, S. R. Rosenberg, S. Nozick, S. J. Green, S. R. Russell, T. A. Poor, T. J. Zak, T. A. Lombardo, T. Stoeger, T. Shamaly,

Z. Ren, Circuits between infected macrophages and T cells in SARS-CoV-2 pneumonia. *Nature*. **590**, 635–641 (2021).

40. T. H. Beacon, G. P. Delcuve, J. R. Davie, Epigenetic regulation of ACE2, the receptor of the SARS-CoV-2 virus. *Genome*. **64**, 386–399 (2021).
41. S. L. Londrigan, K. R. Short, J. Ma, L. Gillespie, S. P. Rockman, A. G. Brooks, P. C. Reading, Infection of Mouse Macrophages by Seasonal Influenza Viruses Can Be Restricted at the Level of Virus Entry and at a Late Stage in the Virus Life Cycle. *J. Virol.* **89**, 12319–12329 (2015).
42. T. Flerlage, D. F. Boyd, V. Meliopoulos, P. G. Thomas, S. Schultz-Cherry, Influenza virus and SARS-CoV-2: pathogenesis and host responses in the respiratory tract. *Nat. Rev. Microbiol.* **0123456789** (2021), doi:10.1038/s41579-021-00542-7.
43. K. D. Hulme, E. C. Noye, K. R. Short, L. I. Labzin, Dysregulated Inflammation During Obesity: Driving Disease Severity in Influenza Virus and SARS-CoV-2 Infections. *Front. Immunol.* **12**, 1–25 (2021).
44. R. C. Coll, J. R. Hill, C. J. Day, A. Zamoshnikova, D. Boucher, N. L. Massey, J. L. Chitty, J. A. Fraser, M. P. Jennings, A. A. B. Robertson, K. Schroder, MCC950 directly targets the NLRP3 ATP-hydrolysis motif for inflammasome inhibition. *Nat. Chem. Biol.* **15**, 556–559 (2019).
45. E. Tsantikos, M. Lau, C. M. N. Castelino, M. J. Maxwell, S. L. Passey, M. J. Hansen, N. E. McGregor, N. A. Sims, D. P. Steinfort, L. B. Irving, G. P. Anderson, M. L. Hibbs, Granulocyte-CSF links destructive inflammation and comorbidities in obstructive lung disease. *J. Clin. Invest.* **128**, 2406–2418 (2018).
46. N. Radhakrishna, M. Farmer, D. P. Steinfort, P. King, A Comparison of Techniques for Optimal Performance of Bronchoalveolar Lavage. *J. Bronchol. Interv. Pulmonol.* **22**, 300–305 (2015).
47. J. Q. Davies, S. Gordon, C. D. Helgason, C. L. Miller, Eds. (Humana Press, Totowa, NJ, 2005; https://doi.org/10.1385/1-59259-838-2:105), pp. 105–116.
48. L. Schimmel, M. van der Stoel, C. Rianna, A. M. van Stalborch, A. de Ligt, M. Hoogenboezem, S. Tol, J. van Rijssel, R. Szulcek, H. J. Bogaard, P. Hofmann, R. Boon, M. Radmacher, V. de Waard, S. Huveneers, J. D. van Buul, Stiffness-Induced Endothelial DLC-1 Expression Forces Leukocyte Spreading through Stabilization of the ICAM-1 Adhesome. *Cell Rep.* **24**, 3115–3124 (2018).
49. T. Dull, R. Zufferey, M. Kelly, R. J. Mandel, M. Nguyen, D. Trono, L. Naldini, A Third-Generation Lentivirus Vector with a Conditional Packaging System. *J. Virol.* **72**, 8463–8471 (1998).
50. M. T. Howes, M. Kirkham, J. Riches, K. Cortese, P. J. Walser, F. Simpson, M. M. Hill, A. Jones, R. Lundmark, M. R. Lindsay, D. J. Hernandez-Deviez, G. Hadzic, A. McCluskey, R. Bashir, L. Liu, P. Pilch, H. McMahon, P. J. Robinson, J. F. Hancock, S. Mayor, R. G. Parton, Clathrin-independent carriers form a high capacity endocytic sorting system at the leading edge of migrating cells. *J. Cell Biol.* **190**, 675–691 (2010).

FIGURE LEGENDS

Figure 1: SARS-CoV-2 does not trigger inflammatory responses from primary human macrophages.

A: HMDM were infected with SARS-CoV-2 (MOI 5) or stimulated with R848 or transfected pIC for 24h. Cytokines in cell supernatants were analysed by alphaLISA. Each data point represents an individual donor (n = 6-15). Graphs show mean + SEM and significance is indicated by asterisks (one-way ANOVA, Dunnett's multiple comparison test). B: HMDM were challenged with SARS-CoV-2 (MOI 0.5, 5), or transfected pIC. Gene expression at 2 and 24h was analysed by qPCR. Graphs shown mean + SEM, where each data point represents an individual donor (n = 3) and significance is indicated by asterisks: $p \leq 0.05$ (*), $p \leq 0.001$ (**), $p \leq 0.0001$ (***) (two-way ANOVA, Dunnett's multiple comparison test).

Figure 2: Primary human monocyte-derived or airway macrophages isolated from bronchoalveolar lavage (BAL) do not support SARS-CoV-2 replication.

A-B: Calu3 cells (A) or HMDM (B) were infected as indicated and virus was left on the cells. Viral RNA isolated from cells was measured by qPCR. Graphs show mean + SEM and each individual point represents an independent experiment (Calu3; n =3) or independent donors (HMDM; n = 7). Significance is indicated by asterisks: $p \leq 0.05$ (*), $p \leq 0.001$ (**), $p \leq 0.0001$ (***) (two-way ANOVA, Tukey's multiple comparison test). C-D: Immunoblots of Calu3 cells (C) or HMDM (D) that were infected as indicated, with virus remaining on the cells. Blot is representative of three independent experiments (Calu3) or three independent donors (HMDM). E-F: BAL macrophages (MOI 1) or Vero cells (MOI 0.5) were infected with SARS-CoV-2 for 1 h, before virus was removed and cell-associated viral RNA (E) or viral RNA released in cell-free supernatants (F) was analysed by qPCR of SARS-CoV-2 E gene at 2 and 48 h post-infection. Data are mean + SEM, with each individual point representing an individual donor (BAL macrophages; n=5) or independent experiments (VERO; n=2). Significance is indicated by asterisks: $p \leq 0.05$ (*), $p \leq 0.001$ (**), $p \leq 0.0001$ (***) (one-way ANOVA, Tukey's multiple comparison test).

Figure 3: Macrophage susceptibility to SARS-CoV-2 requires ACE-2 expression.

A: HMDM and THP-1 cells were analysed by qPCR for ACE2 mRNA expression, with each data point showing an independent donor or experiment (n=3). B: HMDM were stimulated with IFNβ (10 ng/ml) for 6 h and protein extracts were analysed by immunoblot, alongside extracts from THP-1 cells (WT, THP-1-ACE2, THP-1-mSc). C: BAL macrophages from 3 donors were adhered overnight and lysed. Expression of ACE2 in BAL macrophages was analysed by immunoblot, relative to a loading control (Calnexin). Lysate from A549-cells overexpressing ACE2 were used as a positive control. D-E: Cells were infected with SARS-CoV-2 at MOI 0.5 or MOI 5. After 1h the virus inoculum was removed, cells were washed and cells or supernatants harvested at the indicated times. Cellular viral mRNA was analysed by qPCR (D-E), and infectious virions released into cell supernatants were measured by plaque assay (F-G). Data show the mean + SEM of 3-5 independent experiments, with data points representing individual experiments. Significance is indicated by asterisks: $p \leq 0.05$ (*), $p \leq 0.001$ (**), $p \leq 0.0001$ (***) (two-way ANOVA, Tukey's multiple comparison test).

Figure 4: Macrophages can take up SARS-CoV-2 independently of ACE2

A-D: Transmission Electron Microscopy of indicated cells infected with SARS-CoV-2 (MOI 20) at indicated timepoints. For low magnification images (A,C) scale bar = 10 μm, for all other images (A', B, C', D) scale bar = 500 nm.

Figure 5: Macrophage ACE2 expression potentiates macrophage inflammatory responses to SARS-CoV-2

A-B: THP-1-ACE-2 and THP-1-mSc cells (A) or Calu3 cells (B) were infected with SARS-CoV-2 at MOI 5. After 1 h incubation, the virus was removed, and the media replaced. Cells were harvested at the indicated times and gene expression was quantified by qPCR. Gene expression at each time point is presented relative to the mock control to show fold gene induction. Data are mean + SEM of 4 independent experiments (indicated by individual data points) and significance is indicated by asterisks: $p \leq 0.05$ (*), $p \leq 0.001$ (**), $p \leq 0.0001$ (***) (two-way ANOVA, Tukey's multiple comparison test).

Figure 6: Blocking cytokine signalling in ACE2-macrophages rescues productive virion release

A: THP-1 cells were infected with SARS-CoV-2 (MOI 5), which was washed away after 1 h, and incubated for a further 72h, after which cell death was analysed by ATPlite assay. Data are presented as cell viability relative to mock, and are mean + SEM of 3 independent experiments. Significance is indicated by asterisks: $p \leq 0.05$ (*), $p \leq 0.001$ (**), $p \leq 0.0001$ (***) (two-way ANOVA, Tukey's multiple comparison test). B: Schematic of TBK1 (BX-795) inhibition. C-F: THP-1-ACE2 or Calu3 cells were stimulated with SARS-CoV-2 at MOI 5. After 1 h, the viral inoculum was removed and BX-795 added. Supernatants were harvested at 72 h and CXCL10 was analysed by ELISA (C) and viral titres were analysed by plaque assay (D,E). Data show mean + SEM of at least 3 independent experiments, with each individual data point representing a different experiment. Significance is indicated by asterisks: $p \leq 0.05$ (*), $p \leq 0.001$ (**), $p \leq 0.0001$ (***) (C: one-way ANOVA, Tukey's multiple comparison test; D,E: ratio-paired t-test).

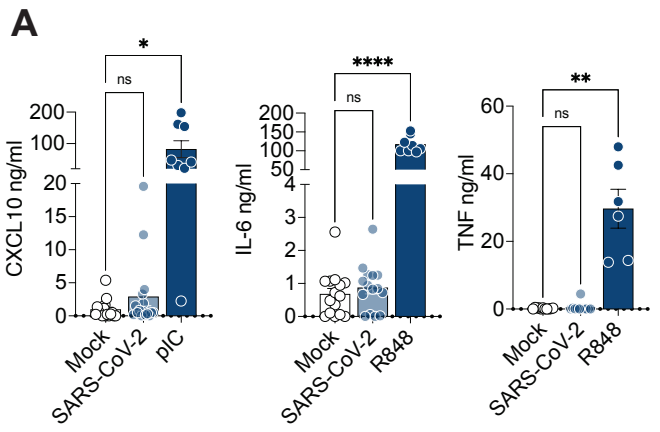

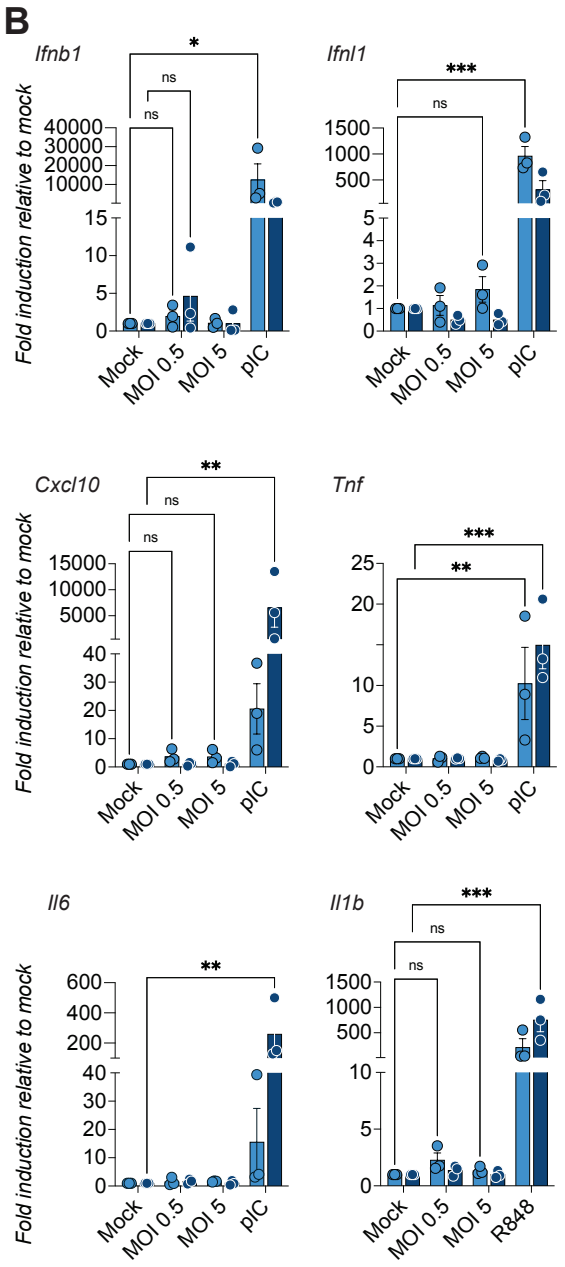

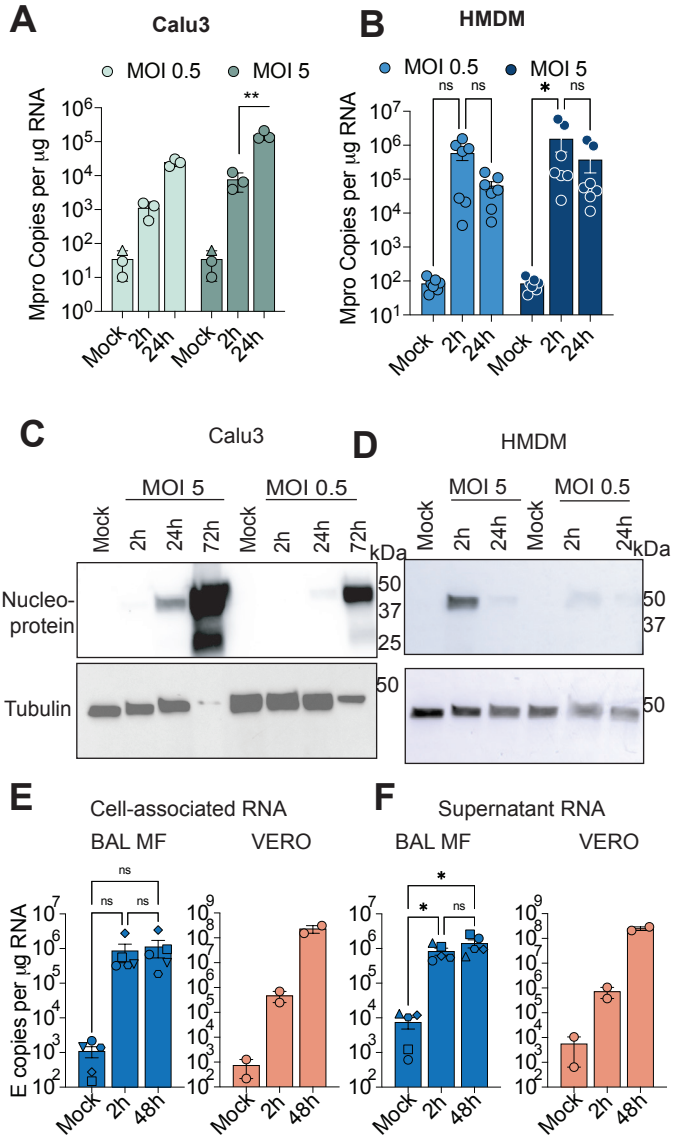

Figure 3

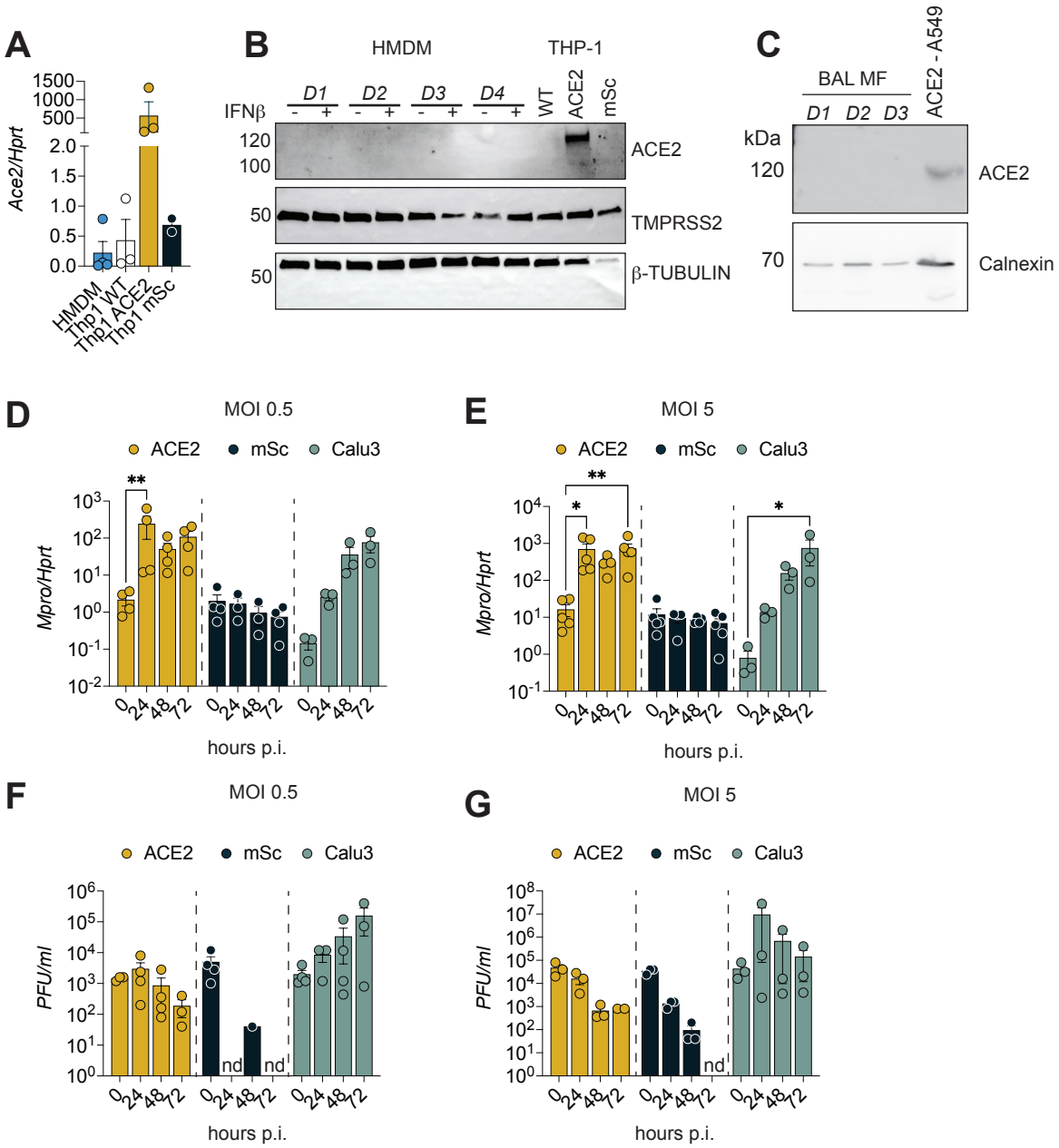

Figure 4

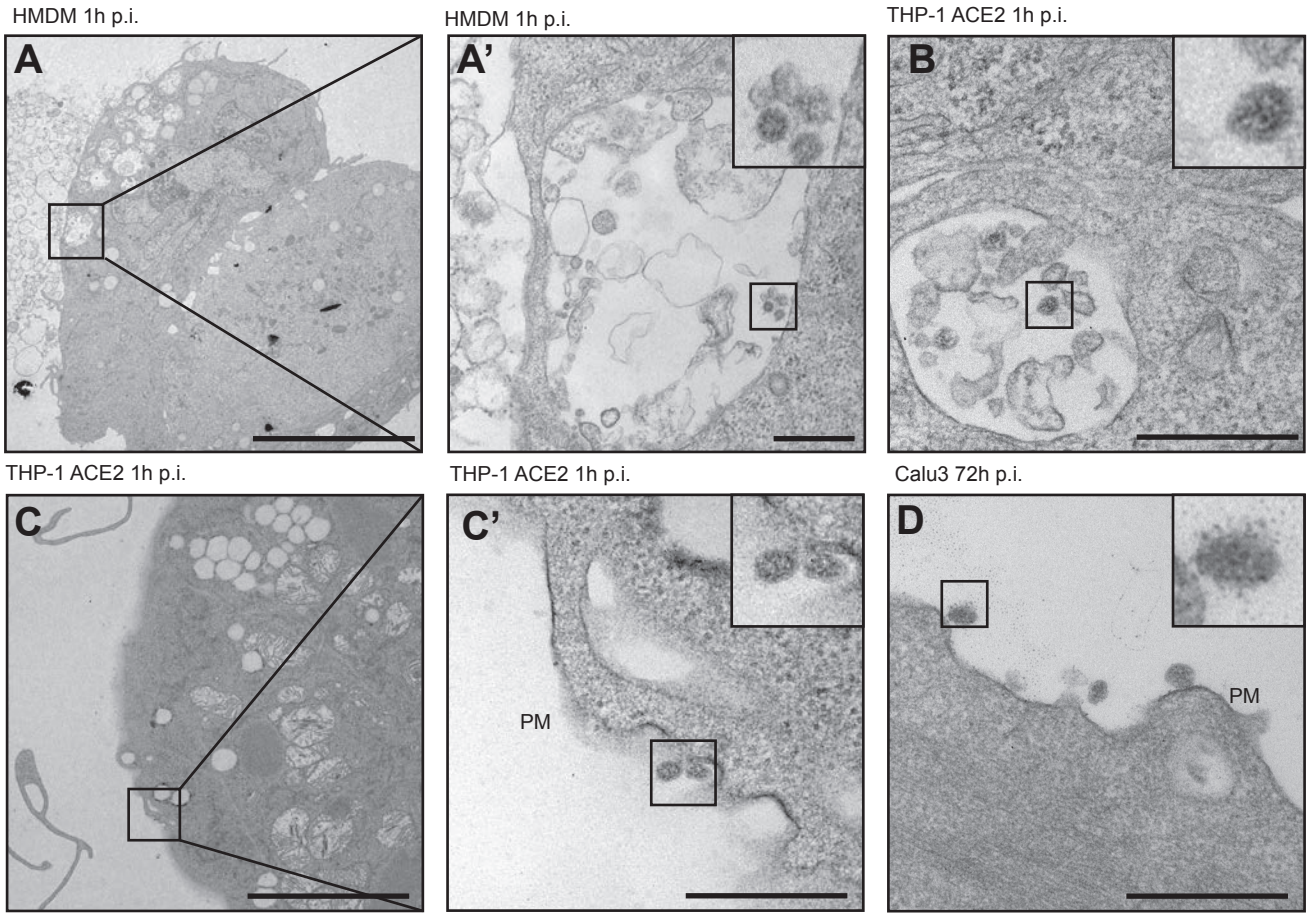

Figure 5

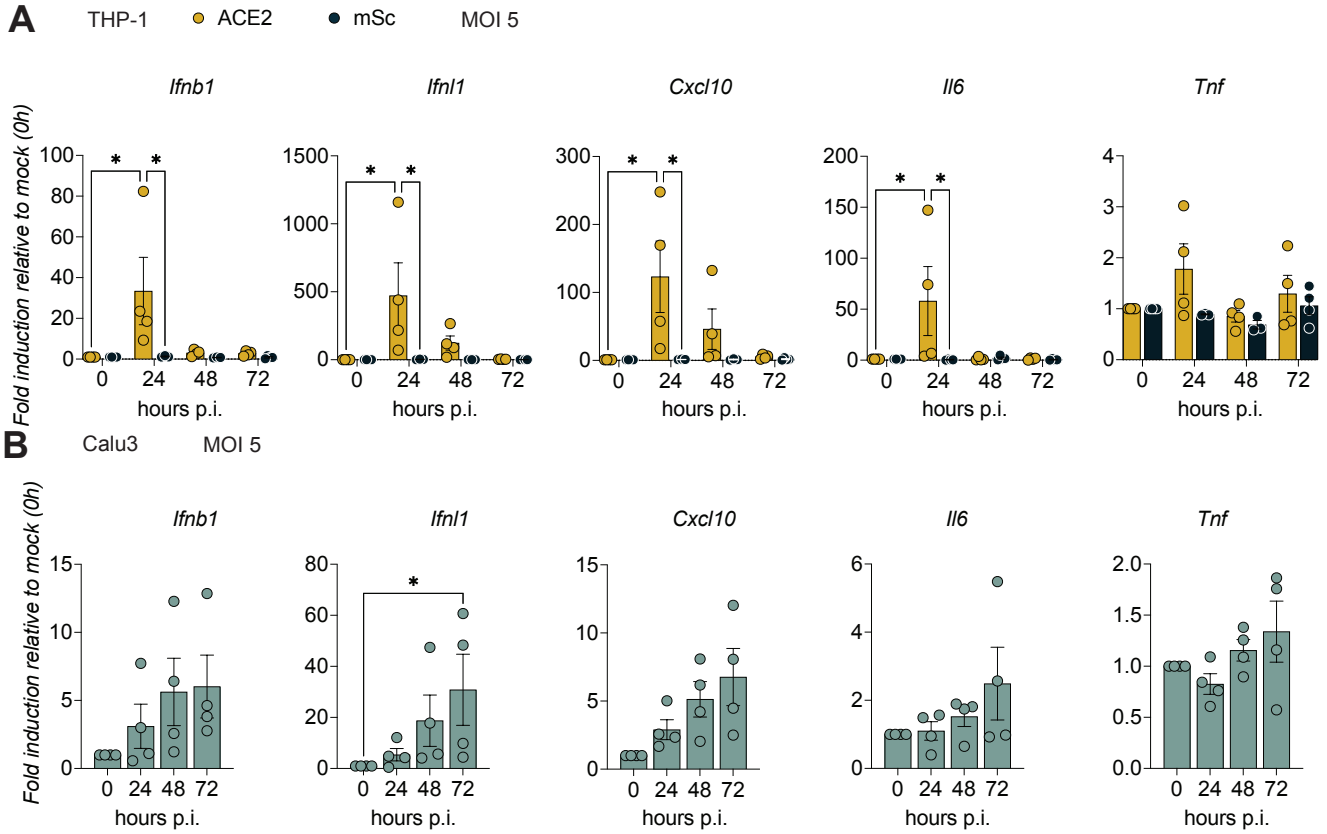

Figure 6